Electronic Supplementary Material (ESI) for Analyst.
This journal is © The Royal Society of Chemistry 2019

Electronic Supplementary Information

Dual-binding pyridine and rhodamine B conjugate derivatives as fluorescent chemosensors for Ferric ion in aqueous media and living cells

Fan Song,[a] Chao Yang,[b] Haibo Liu,[c] Zhigang Gao,[c] Jing Zhu,*[b] Xiaofeng Bao*[c] and Chun Kan*[a]

[a] College of Science, Nanjing Forestry University, Nanjing 210037, China.
[b] Department of Pharmacy, Jiangsu Key Laboratory for Pharmacology and Safety Evaluation of Chinese Materia Medica, Nanjing University of Chinese Medicine, Nanjing 210023, China.
[c] School of Environmental and Biological Engineering, Jiangsu Key Laboratory of Chemical Pollution Control and Resources Reuse, Nanjing University of Science and Technology, Nanjing 210094, China.

Contents

1. Materials and General Methods.

All reagents and organic solvents were of ACS grade or higher and were used without further purification. Unless otherwise noted, all chemicals were purchased from J&K Scientific (Shanghai, China) and were used as received. All solvents were of analytical grade, and double-distilled water was used in all of the experiments. The salts used in the stock solutions of metal ions were $CdCl_2·2.5H_2O$, $CuCl_2·2H_2O$, $AlCl_3$, KNO_3, $FeCl_3·6H_2O$, $HgCl_2$, $NiCl_2·6H_2O$, $MgCl_2·6H_2O$, NaCl, $ZnCl_2$, $CrCl_3·6H_2O$, $Ba(NO_3)_2$, $MnCl_2·4H_2O$, $CoCl_2·6H_2O$, $CaCl_2$ and $PbCl_2$. The reactions were performed under an argon atmosphere using standard Schlenk techniques. Thin-layer chromatography was performed on a HAIYANG silica gel F254 plate and compounds were visualized under UV light (λ=254nm). Column chromatography was performed using HAIYANG silicagel (type: 200–300 mesh ZCX-2).

^1H (500 MHz) and ^{13}C NMR (126 MHz) spectra were recorded on an Avance 500 spectrometer (Bruker; Billerica, MA, USA). The chemical shifts are reported in δ units (ppm) downfield relative to the chemical shift of tetramethyl silane. The abbreviations br, s, d, t, and m denote broad,singlet, doublet, triplet, and multiplet, respectively. Mass spectra were obtained with a Finnigan TSQ Quantum LC/MS spectrometer. High-resolution mass spectra (HRMS) were acquired under electron ionization conditions with a double-focusing high-resolution instrument (Autospec; Micromass Inc.). The pH levels of stock solutions were measured using a PHS-25C Precision pH/mV meter (Aolilong, Hangzhou, China). UV–vis and fluorescence spectra were obtained on a UV-3600 UV-vis-NIR spectrophotometer (Shimadzu, Japan) and an Edinburgh FLS920 fluorescence spectrophotometer (Livingston, UK), respectively, at room temperature. Cell imaging was performed with an inverted fluorescence microscope (OLYMPUS, IX83).

2. Synthesis.

Synthesis of Compound 1

Ethylenediamine (1.3mL, 20mmol.) was added to a solution of rhodamine B (960mg, 2mmol) in ethanol (20 mL). The mixture was refluxed for 12h and then evaporated to dryness under a vacuum. The residue was dissolved in CH_2Cl_2 and then washed with H_2O and brine. The organic layer was dried with $MgSO_4$. After removal of the solvent, flash chromatography (silica gel; MeOH/CH_2Cl_2= 3/97, v/v) of the residue yielded 1 as a pink solid (880mg, 92%). ^1H NMR($CDCl_3$), δ7.90 (dd, J=5.6, 3.0Hz, 1H), 7.61-7.38(m, 2H), 7.09 (dd, J=5.6, 2.9Hz, 1H), 6.43 (d, J=8.8Hz, 2H), 6.37(d, J=2.5Hz,2H), 6.27 (dd, J=8.9, 2.6Hz, 2H), 3.38-3.27 (m, 8H), 3.19 (t, J_1=6.65Hz, J_2=6.6Hz, 2H), 2.41 (t, J_1=6.65Hz, J_2=6.6Hz, 2H), 1.16 (t, J_1=7.0Hz, J_2=7.1Hz, 12H) ppm. ^{13}C NMR ($CDCl_3$), δ168.59, 153.35, 148.79, 132.38, 131.20, 128.64, 128.02, 123.80, 122.71,108.13, 105.65, 97, 64.91, 44.36, 44.06, 40.73, 12.56 ppm. ESI-MS $(M+H)^+$ found, 485.29; calculated for $C_{30}H_{37}N_4O_2$, 484.64.

Synthesis of RBPO

2-Picolinic acid (90mg, 0.73mmol)、N,N'-Dicyclohexylcarbodiimide (DCC, 430mg, 2.09mmol)、1-Hydroxybenzotriazole (HOBt, 280mg, 2.07mmol)、N,N-Diisopropylethylamine (DIPEA, 280μL, 2.17mmol) was dissolved in 30mL of dry CH_2Cl_2. The mixture was stirred at room temperature for 1h. To a

solution of 1 (330mg, 0.68mmol) was added to the mixture above. The mixture was stirred at room temperature for 2h, and the solvent was removed in a vacuum. The residue was dissolved in CH_2Cl_2 and then washed with H_2O. The organic phase was dried with Magnesium sulfate and then concentrated. The residue was purified by column chromatography using petroleum ether/ethyl acetate (4:6, v/v) as an eluent to give **RBPO** as an orange solid (235mg, 61%). ^{1}H NMR ($CDCl_3$), δ8.66 (s, 1H), 8.60(d, J=4.1Hz, 1H), 8.10 (d, J=7.8Hz, 1H), 7.94 (s, 1H), 7.78 (t, J=7.7Hz, 1H), 7.43 (s, 2H), 7.37 (t, J=6.0Hz, 1H), 7.07 (s, 1H), 6.47 (d, J=8.6Hz, 2H), 6.38 (s, 2H), 6.24 (d, J=8.1Hz, 2H), 3.49 (s, 2H), 3.42 (d, J=5.4Hz, 2H), 3.32 (dd, J=6.5, 5.4Hz, 8H), 1.16 (t, J=6.7Hz, 12H) ppm. ^{13}C NMR ($CDCl_3$), δ171.13, 169.22, 164.45, 153.58, 150.17, 148.56, 136.98, 132.55, 130.66, 128.28, 125.77, 122.93, 108.19, 105.10, 97.81, 77.10, 65.27, 60.38, 53.46, 48.88, 44.33, 39.60, 33.96, 25.33, 21.04, 12.60 ppm. ESI-MS $(M+H)^+$ found, 590.31; calculated for $C_{36}H_{39}N_5O_3$, 589.74.

Synthesis of RBPF

To a solution of 1 (212mg, 0.44mmol) in 10mL of dry CH_2Cl_2 was added pyridine-2,6-dicarbonyl dichloride (37mg, 0.18mmol) and triethylamine (46μL, 0.32mmol). The mixture was stirred at room temperature for 3h, and the solvent was removed in a vacuum. The residue was dissolved in CH_2Cl_2 and then washed with H_2O. The organic phase was dried with Magnesium sulfate and then concentrated. The residue was purified by column chromatography using 0.3% MeOH/CH_2Cl_2 as an eluent to give **RBPF** as an orange solid (136mg, 55%). ^{1}H NMR ($CDCl_3$), δ8.19 (d, J=7.8Hz, 2H), 8.02(d, J=7.5Hz, 2H), 7.89 (t, J_1=7.7Hz, J_2=7.8Hz, 1H), 7.41-7.52 (m, 4H), 7.07 (d, J=7.5Hz, 2H), 6.51 (d, J=8.9, 4H), 6.38 (s, 4H), 6.23 (dd, J=8.9, 3.6Hz, 4H), 3.58 (d, J=6.0Hz, 4H), 3.40 (d, J=5.4Hz, 4H), 3.25-3.32 (m, 16H), 1.14 (s, 24H) ppm. ^{13}C NMR ($CDCl_3$), δ168.67, 163.01, 152.71, 147.65, 137.26, 131.59, 129.30, 122.67, 107.25, 104.27, 97, 64.67, 52.49, 43.35, 39.10, 30.95, 28.72, 21.72, 11.68 ppm. ESI-MS $(M+H)^+$ found, 1100.57; calculated for $C_{67}H_{73}N_9O_6$, 1100.38.

3. NMR and MS spectra.

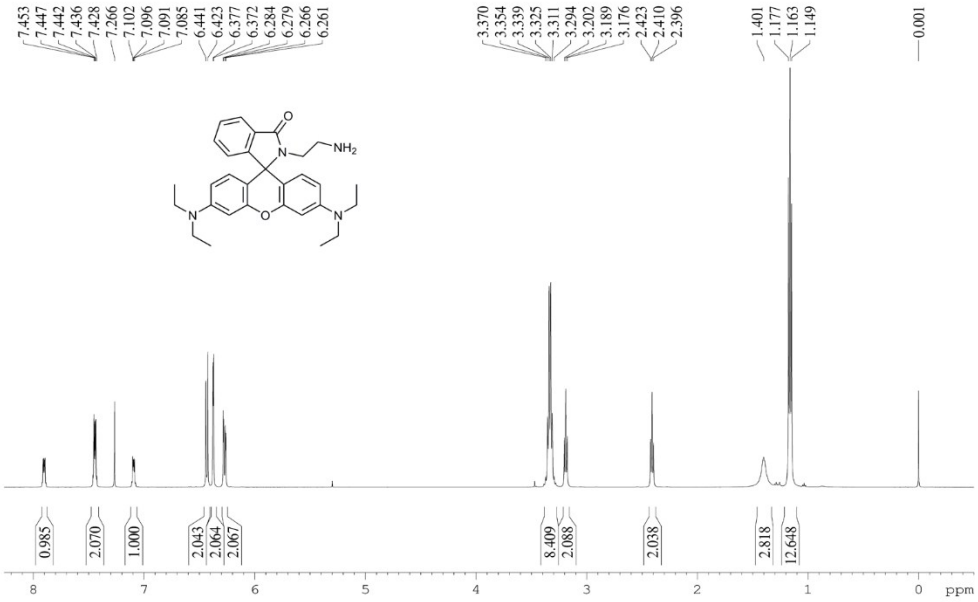

Fig. S-1 ^{1}H NMR ($CDCl_3$, 500 MHz) spectra of compound 1.

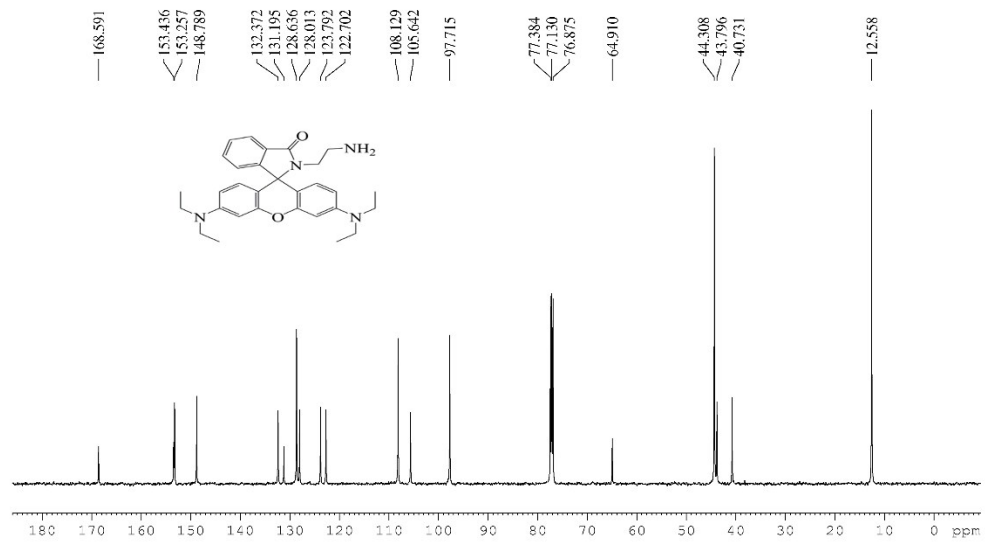

Fig. S-2 ^{13}C NMR ($CDCl_3$,125 MHz) spectra of compound 1.

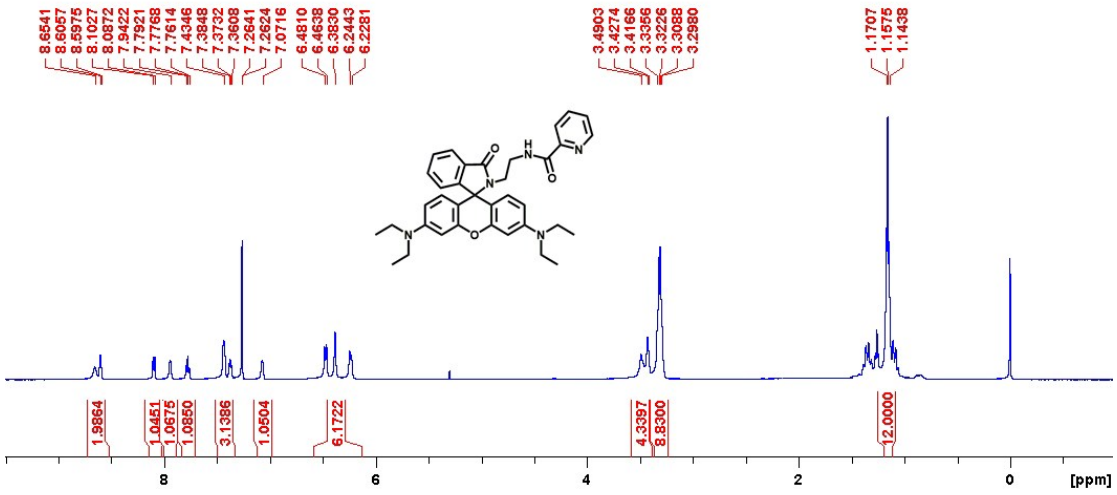

Fig. S-3 ^{1}H NMR ($CDCl_3$, 500 MHz) spectra of compound RBPO.

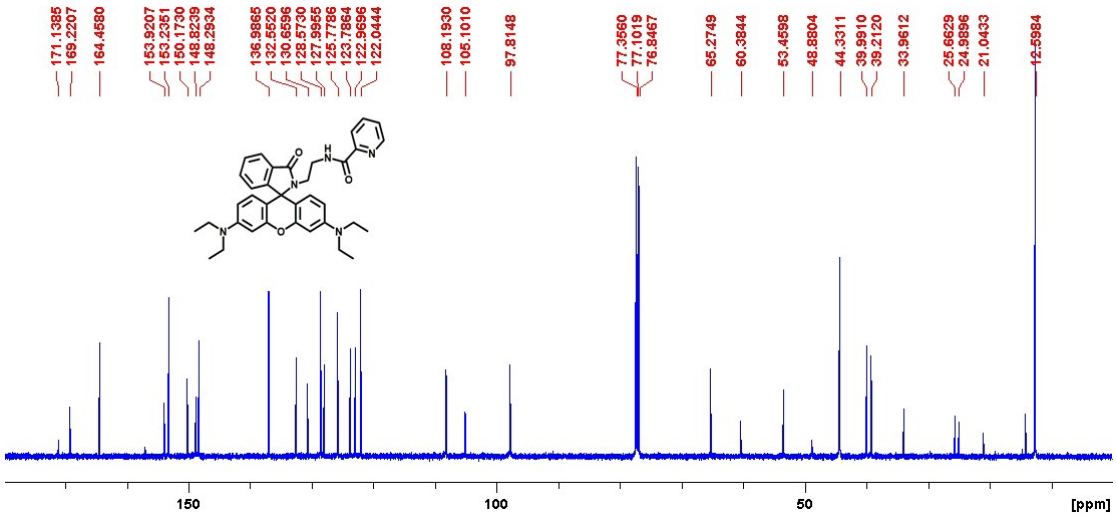

Fig. S-4 ^{13}C NMR ($CDCl_3$, 125 MHz) spectra of compound RBPO.

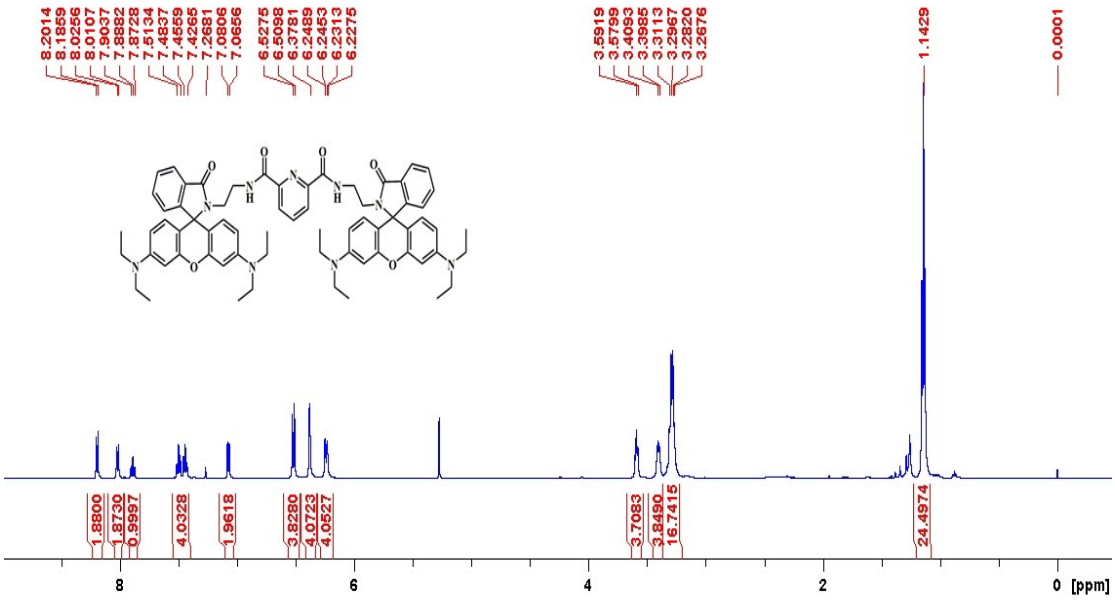

Fig. S-5 ^{1}H NMR ($CDCl_3$, 500 MHz) spectra of compound RBPF.

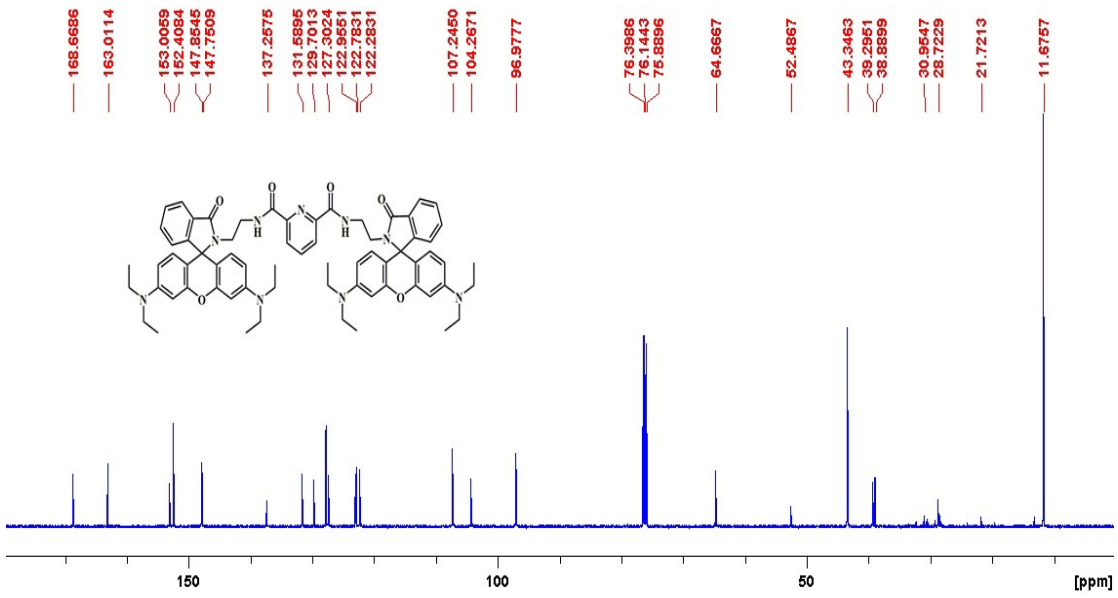

Fig. S-6 ^{13}C NMR ($CDCl_3$, 125 MHz) spectra of compound RBPF.

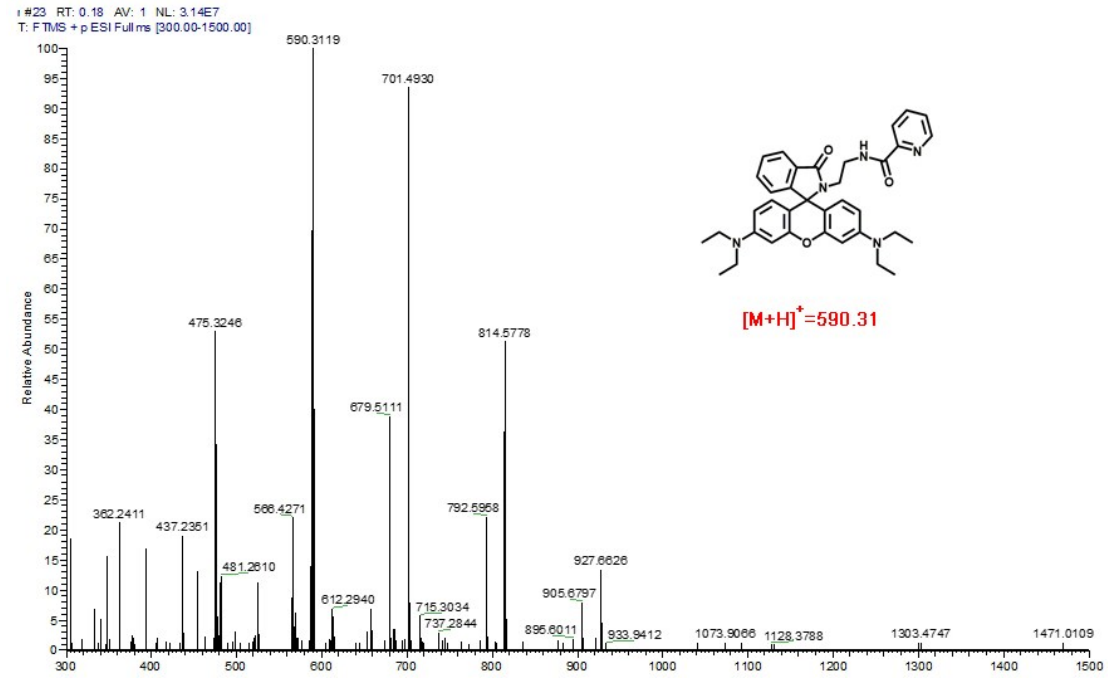

Fig. S-7 ESI-MS spectrum of compound RBPO.

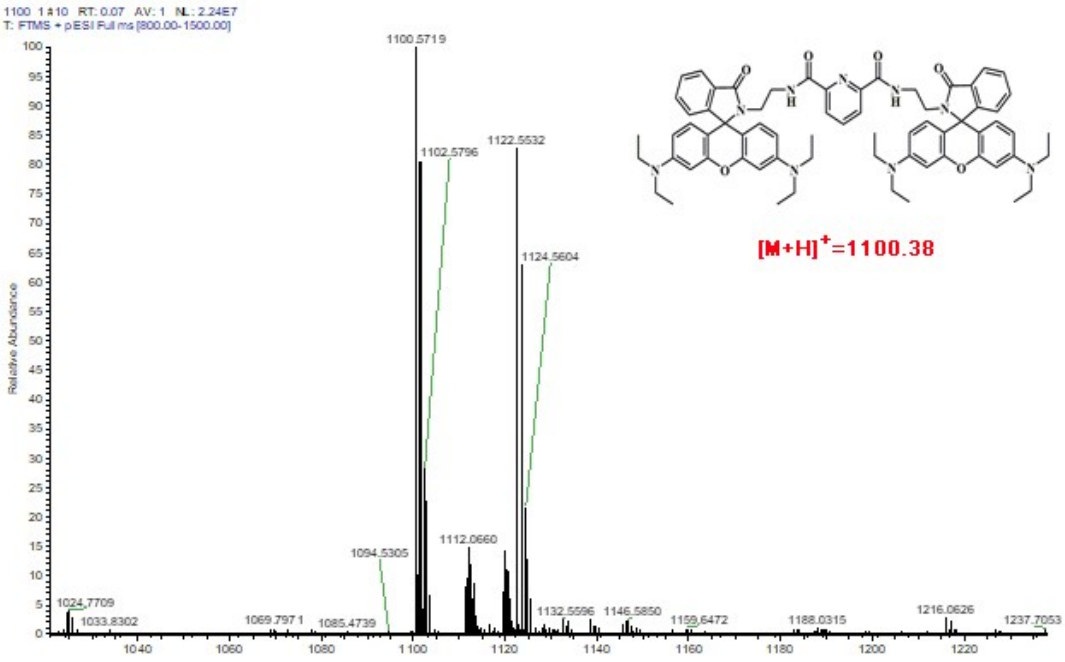

Fig. S-8 ESI-MS spectrum of compound RBPF.

4. Experiment graphs and Tables.

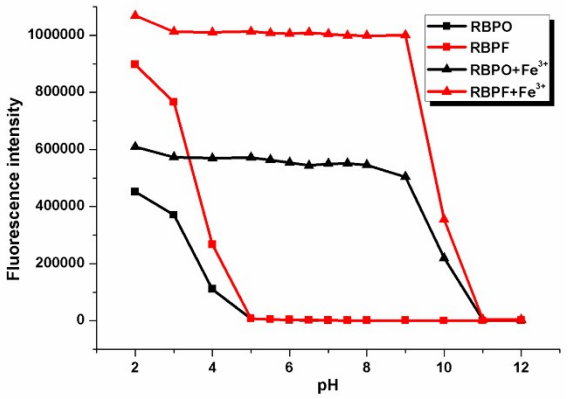

Fig. S-9 Effect of pH on the fluorescence of RBPO (20μM) and RBPF (20μM) in EtOH/H_2O solutions (3:1, v/v) in the absence and presence of Fe^{3+} (100μM). The excitation and emission wavelengths were 560 nm and 582 nm, respectively.

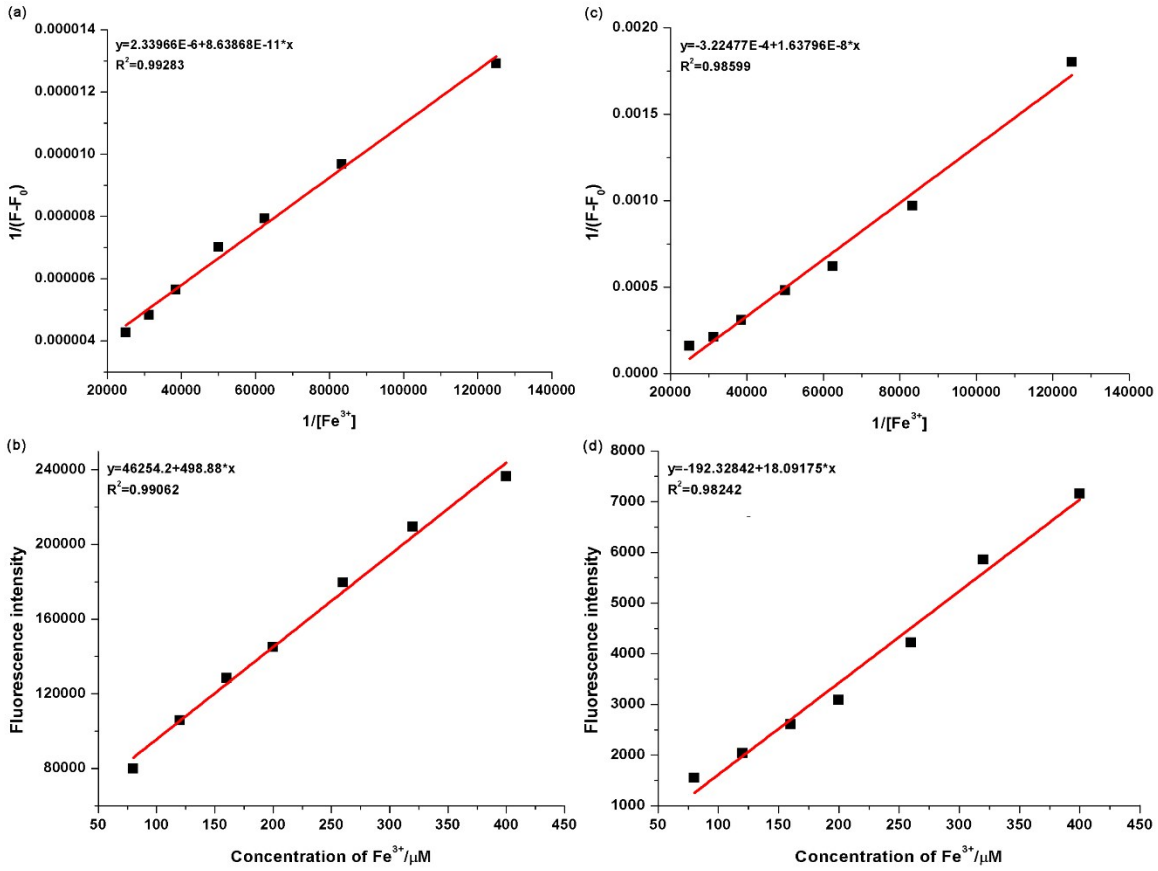

Fig. S-10 (a, c) Benesi-Hildebrand plot (λ_{em} = 582 nm) of 1/(F-F_0) vs 1/[Fe^{3+}]. Fluorescent intensity at 582 nm of (b) RBPO (20μM) and (d) RBPF (20μM) 8989, HEPES, 0.5Mm, pH=7.33) with different amounts of Fe^{3+}. The excitation wavelength is 560 nm.

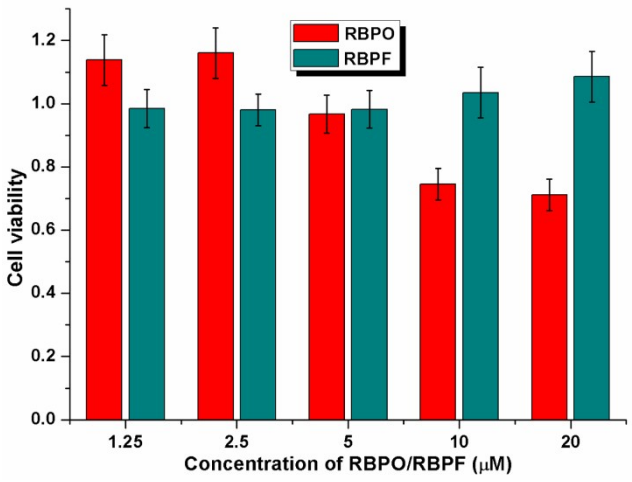

Fig. S-11 Cytotoxicity assay of chemosensors RBPO and RBPF for human breast adenocarcinoma (MCF-7) cells by the MTT test. Human breast adenocarcinoma (MCF-7) cells were respectively cultured in the presence of different concentrations of RBPO and RBPF (1.25, 2.5, 5, 10, and 20 μM) at 37 °C for 24h. For the control group, human breast adenocarcinoma (MCF-7) cells were incubated under the same conditions but without chemosensors RBPO or RBPF.

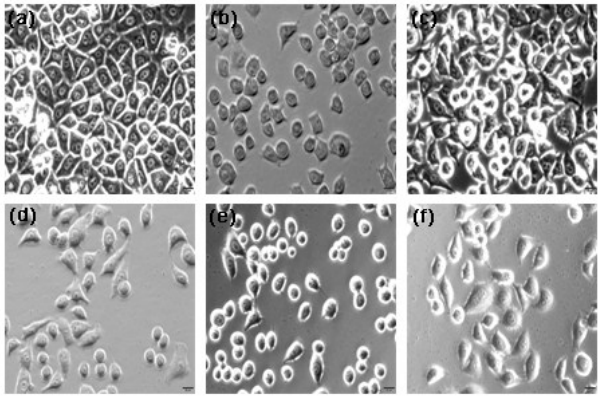

Fig. S-12 Bright field of cells treated with no RBPO (a), RBPF (d) or Fe^{3+}. Cells incubated with (b) RBPO (10μM) and (e) RBPF (10μM) in the bright field. Cells pretreated with (c) RBPO (10μM) and (f) RBPF (10μM) incubated with Fe^{3+} (100μM) for 2h in the bright field.

Calculation of association constant

The association constant (K_a) of **RBPO**-Fe^{3+} and **RBPF**-Fe^{3+} complexs were determined by Benesi-Hildebrand Formula(1):

$$\triangle F = F - F_0 = \Delta F = \Delta F = [Fe^{3+}](F_{max} - F_0)/\left(1/K_a + [Fe^{3+}]\right) \qquad \textbf{(1)}$$

Where F is the fluorescence intensity at 582 nm upon addition of different concentration of Fe^{3+}, F_0 is the fluorescence intensity at 582 nm in the absence of Fe^{3+} and F_{max} is the saturated intensity at 582 nm in the presence of Fe^{3+}.The association constant (Ka) was evaluated graphically by plotting $1/[F\text{-}F_0]$ against $1/[Fe^{3+}]$. Linear fit to the data according to the formula **(1)**, through the slope and intercept, the

binding constant of **RBPO** was calculated as 2.70×10^4 M^{-1} and the binding constant of **RBPF** was calculated as 1.97×10^4 M^{-1}.

Determination of detection limit

According fluorescence titration experiments, we can also calculate the detection limit of **RBPO** and **RBPF** for Fe^{3+}. The fluorescence intensity of the blank samples was measured for 10 times, calculate the standard deviation of the fluorescence intensity at 582nm. Then, make a curve based on the fluorescence intensity of **RBPO**/**RBPF** at 582 nm and the concentration of Fe^{3+} to obtain the slope. The detection limit was calculated according to the following formula:

$$\text{Detection limit} = \frac{3SD}{S} \quad \textbf{(2)}$$

Where SD is the standard deviation of the blank solution detected for 10 times; S is the slope of the calibration curve. Finally, the detection limit of **RBPO** is calculated to be 0.067μM and the detection limit of **RBPF** is calculated to be 0.345μM.

Tab. S-1 Detailed Calculations for Ka of RBPO-Fe^{3+}.

[Fe^{3+}]（M）	**1/[Fe^{3+}]**	**F**	**F-F_0**	**1/(F-F_0)**
0		2372（F_0）		
0.8E-06	1.25E+05	79828	77456	0.00001291
1.20E-05	8.33E+04	105724	103352	0.00000968
1.60E-05	6.25E+04	128513	126141	0.00000793
2.00E-05	5.00E+04	144932	142560	0.00000701
2.60E-05	3.85E+04	179505	177133	0.00000565
3.20E-05	3.13E+04	209391	207019	0.00000483
4.00E-05	2.50E+04	236465	234093	0.00000427

Tab. S-2 Detailed Calculations for Ka of RBPF-Fe^{3+}.

[Fe^{3+}]（M）	**1/[Fe^{3+}]**	**F**	**F-F_0**	**1/(F-F_0)**
0		998（F_0）		
0.8E-06	1.25E+05	1552	554	0.00180
1.20E-05	8.33E+04	2033	1035	0.00097
1.60E-05	6.25E+04	2609	1611	0.00062
2.00E-05	5.00E+04	3086	2088	0.00048
2.60E-05	3.85E+04	4223	3225	0.00031
3.20E-05	3.13E+04	5854	4856	0.00021
4.00E-05	2.50E+04	7158	6160	0.00016

Tab. S-3 Calculations of SD (RBPO).

F.I. of the blank solution		$X_i-\overline{X}$ (i=1,2,3,4,5,6,7,8,9,10)	$(X_i-\overline{X})^2$		SD
X_1	2372	19	Y_1	361	
X_2	2356	3	Y_2	9	
X_3	2361	8	Y_3	64	
X_4	2338	-15	Y_4	225	
X_5	2363	10	Y_5	100	
X_6	2345	-8	Y_6	64	
X_7	2339	-14	Y_7	196	
X_8	2350	-3	Y_8	9	
X_9	2359	6	Y_9	36	
X_{10}	2347	-6	Y_{10}	36	
average value $\overline{X}$	2353		$SD^2=(Y_1+Y_2+Y_3+Y_4+Y_5+Y_6+Y_7+Y_8+Y_9+Y_{10})/9$	122.2	11.05

Tab. S-4 Calculations of SD (RBPF).

F.I. of the blank solution		$X_i-\overline{X}$ (i=1,2,3,4,5,6,7,8,9,10)	$(X_i-\overline{X})^2$		SD
X_1	998	3.1	Y_1	9.61	
X_2	995	0.1	Y_2	0.01	
X_3	993	-1.9	Y_3	3.61	
X_4	996	1.1	Y_4	1.21	
X_5	991	-3.9	Y_5	15.21	
X_6	995	0.1	Y_6	0.01	
X_7	997	2.1	Y_7	4.41	
X_8	995	0.1	Y_8	0.01	
X_9	993	-1.9	Y_9	3.61	
X_{10}	996	1.1	Y_{10}	1.21	
average value $\overline{X}$	994.9		$SD^2=(Y_1+Y_2+Y_3+Y_4+Y_5+Y_6+Y_7+Y_8+Y_9+Y_{10})/9$	4.32	2.08

$$SD=\sqrt{\frac{1}{N-1}\sum_{i=1}^{N}(X_i-\bar{X})^2}$$

Tab. S-5 Determination of the recovered Fe^{3+} concentration in tap water samples by fluorescent method using RBPO (20μM) and RBPF (20μM).

Sample	Amount of spiked Fe^{3+} (μM)	Fe^{3+} found (μM)	Recovery (%)
1+**RBPO**	33	30.41	92.15
2+**RBPO**	67	61.52	91.82
3+**RBPO**	100	91.82	91.82
4+**RBPO**	133	123.24	92.66
5+**RBPO**	167	152.81	91.50
6+**RBPO**	200	188.33	94.16
1+**RBPF**	33	30.06	91.09
2+**RBPF**	67	62.47	93.24
3+**RBPF**	100	91.28	91.28
4+**RBPF**	133	120.11	90.31
5+**RBPF**	167	151.59	90.77
6+**RBPF**	200	189.13	94.57